

## Improved metabolic stability and therapeutic efficacy of a novel molecular gemcitabine phospholipid complex



Chander Parkash Dora<sup>a,b</sup>, Varun Kushwah<sup>a</sup>, Sameer S. Katiyar<sup>a</sup>, Pradeep Kumar<sup>c</sup>, Viness Pillay<sup>c</sup>, Sarasija Suresh<sup>d,e</sup>, Sanyog Jain<sup>a,\*</sup>

<sup>a</sup> Centre for Pharmaceutical Nanotechnology, Department of Pharmaceutics, National Institute of Pharmaceutical Education and Research (NIPER), S.A.S. Nagar, Punjab, 160062, India

<sup>b</sup> Department of Pharmaceutical Technology (Formulations), National Institute of Pharmaceutical Education and Research (NIPER), S.A.S. Nagar, Punjab, 160062, India

<sup>c</sup> Wits Advanced Drug Delivery Platform Research Unit, Department of Pharmacy and Pharmacology, School of Therapeutic Sciences, Faculty of Health Sciences, University of the Witwatersrand, Johannesburg, Parktown 2193, South Africa

<sup>d</sup> Institute for Drug Delivery and Biomedical Research (IDBR), Bangalore, Karnataka, 560068, India

<sup>e</sup> RGV Research & Innovations Pvt. Ltd (RGVRI), Bangalore, Karnataka, 560010, India

### ARTICLE INFO

#### Article history:

Received 20 April 2017

Received in revised form 18 July 2017

Accepted 20 July 2017

Available online 21 July 2017

#### Keywords:

Gemcitabine

Phospholipid complex

Lipid solubility

Stability

Anticancer

Pancreas adenocarcinoma

### ABSTRACT

The aim of the present research is to increase lipid solubility, metabolic stability and therapeutic efficacy of water soluble gemcitabine (GEM) via phospholipid complex (PC) formation. A novel phospholipid complex of GEM was successfully prepared and optimized. Physical interaction of GEM with phospholipid was evaluated by DSC, FT-IR, <sup>1</sup>H NMR, <sup>31</sup>P-NMR and P-XRD. SEM images of GEM-PC showed rough structure and TEM images of diluted aqueous dispersion of GEM-PC showed micellar structure. *In silico* study also revealed the significant interaction between drug and phospholipid. GEM-PC demonstrated sustained drug release pattern and high plasma stability (~2.2 fold) *in vitro* as compared to GEM. Increased *in vitro* cytotoxicity and apoptosis were observed with GEM-PC, when incubated with human pancreas adenocarcinoma cell lines. *In vivo* pharmacokinetics showed the almost 2 fold increase in AUC<sub>0-∞</sub> (area under curve) with phospholipid complex (8983.26 ng h/ml) as compared with GEM (4371.18 ng h/ml) and GEMITA (4689.29 ng h/ml). Toxicity studies signify the safety of GEM-PC over GEMITA. Pharmacodynamics studies in pancreatic tumor model further revealed higher efficacy of GEM-PC than GEMITA. These findings suggested the higher potential of phospholipid based technology for the enhancement of metabolic stability and therapeutic efficacy of GEM.

© 2017 Elsevier B.V. All rights reserved.

### 1. Introduction

Gemcitabine (2',2'-Difluorodeoxycytidine; dFdC, GEM) is a deoxycytidine nucleoside analogue with a wide spectrum of cytotoxic activity against pancreatic, breast, lung, and ovarian cancer (Pappas et al., 2006). It is an antimetabolite prodrug, which actively transports through the human nuclear transport receptor and converts into an active 5'-triphosphate derivative of GEM. It induces an S-phase arrest, inhibits DNA synthesis by incorporation into DNA and inhibits its elongation. It also inhibits ribonucleotide reductase enzyme. It is rapidly converted into the inactive metabolite 2'-deoxy-2', 2'-diflurouridine (dFdU) by cytidine

deaminase in blood, liver, kidney and other tissues. The biggest hurdle associated with the current clinical treatment with GEM is its very short plasma half life (~45 min) (Immordino et al., 2004). To overcome this hurdle, it is usually administered at higher dose via i.v route which increases dose dependent toxicity that includes severe haematological toxicity, and toxicity related to highly perfused organs such as liver and kidney (Dasanu, 2008). Several efforts have already been reported to prolong the release and *in vivo* stability of GEM. These include PEGylation (Vandana and Sahoo, 2010), polypeptide conjugation (Kiew et al., 2010), bioconjugation (Jain et al., 2014b), chitosan nanoparticles (Arias et al., 2011), and prodrug-nanoparticles (Sloat et al., 2011). Although various lipids conjugates of GEM (Daman et al., 2014; Desmaële et al., 2012; Paolino et al., 2010) have also shown higher efficacy and lesser toxicity as compared to only free drug administration, but failed to enter in the market as a commercial treatment. Overall, several issues e.g. stability, entrapment

\* Corresponding author at: Center for Pharmaceutical Nanotechnology, Department of Pharmaceutics, NIPER, Sec-67, S.A.S. Nagar, Punjab, 160062, India.

E-mail addresses: [sanyogjain@niper.ac.in](mailto:sanyogjain@niper.ac.in), [sanyogjain@rediffmail.com](mailto:sanyogjain@rediffmail.com) (S. Jain).

efficiency, toxicity were not covered by any single previously reported formulation (Joshi et al., 2014). Now, here we tried to circumvent these problems by phospholipid complex.

Due to structure similarity of phospholipid (which are amphipathic molecules), with the mammalian cell membrane; they possess themselves a suitable carrier in drug delivery technology with good biodegradable and biocompatible potential. Phospholipid complex technology has been utilized to improve the permeability, water-oil partition coefficient and systemic bioavailability of various drugs (Khan et al., 2013). Phospholipid complex, usually formed by dissolving phospholipids in non-aqueous solvents, has shown a good means of affinity for both, hydrophilic as well as hydrophobic drugs. These amphiphilic drug lipid complexes are stable and more bioavailable drug delivery systems with low interfacial tension between the system and the gastrointestinal fluid, thereby promoting membrane, tissue and cell wall transfer, in the body.

Several drugs, such as, rifampicin (Singh et al., 2014), tamoxifen (Jena et al., 2014), curcumin (Khatik et al., 2016), resveratrol (Duan et al., 2013), and morin (Zhang et al., 2011) have been reported to have improved their solubility and oral bioavailability through phospholipid complexation phenomenon. At the same time, it is also an important carrier for those drug molecules which need a sustained/controlled release behavior inside the body due to their short half life (Semalty et al., 2009). This phenomenon had also attributed to the lipid solubilization capability of phospholipids facilitating permeability of water soluble drugs through lipidic membrane and thus increasing their therapeutic efficacy, e.g. luteolin (Xu et al., 2009), catechin (Semalty et al., 2012), clarithromycin (Lu et al., 2009), mitomycin C (Hou et al., 2012), vinorelbine (Li et al., 2013), and insulin (Shi et al., 2006).

Here, we demonstrated the formation of molecular complex of phospholipid with water soluble drug. So far, this is the first ever attempt to improve the metabolic stability of GEM by modulating its aqueous solubility. The present work was aimed to develop molecular complex of phospholipid and GEM as a sustained delivery platform by promoting lipid solubility and thus, plasma stability of drug molecule. Initially, the GEM-PC was prepared by solvent evaporation method, which further was suitably characterized by different techniques. *In vitro* cell line assays were implemented to check the cytotoxic potential of GEM-PC. *In silico*, *in vivo* toxicity, *in vivo* pharmacokinetics and finally pharmacodynamics study were also evaluated. We anticipate that phospholipid complex of GEM may be a useful platform for developing new injectable drug delivery system with sustained release behavior.

## 2. Materials and methods

### 2.1. Materials

Gemcitabine hydrochloride was obtained as a gift sample from Mac-Chem Products Pvt. Ltd. (Mumbai, India). Lipoid® S75 was gifted by Lipoid GmbH, (Ludwigshafen, Germany). Sodium hydroxide, sodium chloride, potassium chloride, potassium hydrogen phosphate, disodium hydrogen phosphate and n-octanol were purchased from Himedia labs (Mumbai, India). Tetrahydrofuran was purchased from Alfa-Aeser, (MA, USA). Trichloroacetic acid, 2'-deoxyribonucleic acid, dialysis membrane (10 kDa MWCO), Dulbecco's modified Eagle's medium (DMEM), antibiotic-antimycotic solution, 3-(4,5-dimethylthiazol-2-yl)-2,5-diphenyltetrazolium bromide (MTT), ethylenediaminetetraacetic acid (EDTA), trypsin and sodium acetate were purchased from Sigma-Aldrich Co., St. Louis, MO, USA. Fetal bovine serum (FBS) was procured from Invitrogen™, life technologies, Thermo Fisher Scientific Inc. (USA).

Commercial kits for estimation of Aspartate Aminotransferase (AST), Alanine Aminotransferase (ALT), Blood Urea Nitrogen (BUN) and Creatinine level were purchased from Accurex Biomedical Pvt. Ltd., Mumbai, India. HPLC grade solvents (methanol and acetonitrile) were purchased from Merck Specialities Pvt. Ltd. (Mumbai, India). Purified water (Millipore, Billerica, MA, USA), degassed and filtered through 0.45 µm hydrophilic PVDF filters (Millipore Millex-HV), was used in all experiments. MIA PaCa-2 and PANC-1 (Human Pancreas adenocarcinoma) cell lines were obtained from the cell repository facility of National Centre for Cell Sciences (NCCS), Pune, India. All other reagents, materials, and solvents used were of analytical grade.

### 2.2. Preparation of GEM-phospholipid complex (GEM-PC)

GEM-PC was prepared by solvent evaporation method with slight modifications (Peng et al., 2012). Briefly, different molar ratio (2:1, 1:1, 1:2 and 1:4) of GEM:Phospholipid, and complexing solvent (methanol, ethanol and tetrahydrofuran) were studied for the preparation of GEM-PC. Briefly, GEM and Lipoid® S75 were co-dissolved in selected ratio in 20 ml of optimized solvent and refluxed at 60 °C for 12 h. The solvent was then evaporated using a rotary evaporator (R-210, Buchi, Switzerland) to get the GEM-PC, which was further washed with dichloromethane to separate free GEM and then dried under vacuum for overnight to remove traces of solvents. The resultant complex was stored in airtight container at below 20 °C.

### 2.3. Estimation of drug content in GEM-PC

The amount of GEM in the GEM-PC was determined by validated HPLC method. Accurately weighed quantity of GEM-PC was dissolved in methanol, sonicated for 15 min and analyzed by reverse phase HPLC (RP-HPLC; Waters 2695 separation module, Waters Co., MA, USA) using C18 column (250 mm × 4.6 mm × 5 µm; Thermo Fisher Scientific Inc., USA) and mobile phase (phosphate buffer (pH 3.5, 0.05 M): Methanol; 40:60) with a flow rate of 0.8 ml/min. The injection volume was 20 ml and retention time of GEM was found to be 5.3 min. GEM was estimated at 268 nm ( $\lambda_{\text{max}}$ ) using a PDA detector (Waters 2996 photodiode array, Waters Co., MA, USA).

### 2.4. Characterization of GEM-PC

#### 2.4.1. Differential scanning calorimetry (DSC)

Thermal behavior of pure GEM, phospholipid, GEM-PC, physical mixture of GEM and phospholipid were recorded on a DSC (DSC 821e, Mettler Toledo International Inc., Switzerland) using Mettler Stare system equipped with STARe SW 9.01 software. The temperature axis and cell constant of DSC were previously calibrated with Indium. A heating rate of 20 °C/min was employed over a temperature range of 25–300 °C with nitrogen purging (40 ml/min). Samples (2–3 mg) were kept on aluminum pan and analyzed as sealed with pinholes.

#### 2.4.2. Powder X-Ray diffraction (P-XRD) study

The X-ray diffractions of the samples were recorded on a powder X-ray diffractometer (D8 advanced diffractometer, Bruker AXS GmbH, Germany) equipped with EVA software. The standard Bragg-Brentano geometry was used to analyse phase distribution of powdered samples. 40 kV was applied to X-ray tube to maintain current at 40 mA. Cu  $\text{K}_{\alpha}$  (wavelength 1.5406 Å) radiation source was used. The samples were scanned from 4° to 40° 2θ at a scan rate of 0.1° 2θ/min. The samples were irradiated at room temperature. Alignment calibration was made using the Alumina powder.

#### 2.4.3. Fourier transform infrared spectroscopy (FT-IR)

The FT-IR spectra of pure GEM, phospholipid, GEM-PC, physical mixture of GEM and phospholipid were recorded with the FT-IR synthesis monitoring system (Perkin-Elmer Inc., USA) equipped with Spectrum<sup>TM</sup> software (spectrum V5.02 CIC photonics Inc., USA), using the KBr pellet method in the region of 4000–400 cm<sup>-1</sup> (resolution of 4 cm<sup>-1</sup> and 10 number of scans).

#### 2.4.4. Nuclear magnetic resonance (NMR) analyses

**Proton NMR** (<sup>1</sup>H NMR)-Briefly, Phospholipid, GEM-PC and GEM were dissolved in CD<sub>3</sub>OD and D<sub>2</sub>O (99.9 atom% deuterium-enriched, Sigma-Aldrich Inc., USA) respectively. <sup>1</sup>H NMR spectra of GEM, phospholipid and GEM-PC were recorded with employing ZH079807 Bruker 400 UltraShield<sup>TM</sup> spectrophotometer with Bruker B-ACS120 Autosampler and Topspin 2.7 software (Bruker Corporation, USA). Tetramethylsilane (TMS) was used as a reference standard. Chemical shifts ( $\delta$ ) were expressed in ppm relative to TMS.

**Phosphorous NMR** (<sup>31</sup>P NMR)- <sup>31</sup>P NMR spectra of samples were recorded on a ZH079807 Bruker 400 UltraShield<sup>TM</sup> spectrophotometer with Bruker B-ACS120 Autosampler and Topspin 2.7 software (Bruker Corporation, USA) in a 5-mm broad band probe at 25 °C as previously reported (Dhanikula and Panchagnula, 2008). Samples (Phospholipid and GEM-PC) were dissolved in CD<sub>3</sub>OD. 5000–5200 transients were accumulated with a pulse length of 14  $\mu$ s and 1 s relaxation delay.

#### 2.4.5. Morphology

**Scanning electron microscopy (SEM)**-The surface morphology of GEM, phospholipid and GEM-PC was observed by using Hitachi S-3400N scanning microscope (Hitachi High-Technologies Corporation, Japan) at an accelerating voltage of 10 kV. Samples were sputter-coated (E-1010, Hitachi High-Technologies Corporation, Japan) with gold-palladium alloy to minimize the surface charging.

**Transmission electron microscopy (TEM)**-A drop of GEM-PC dispersion (diluted 50x with HPLC grade water) was mounted on the carbon-coated copper grid and stained with phosphotungstic acid (2% w/v). The grid was air dried, and scanned under the transmission electron microscope (FEI Tecnai G2F20, Netherlands) at different magnifications.

#### 2.5. Solubility

Excess amount of GEM, physical mixture and GEM-PC were dissolved in water and n-octanol and kept for 24 h at 25 °C in shaker water bath (EQUITRON®, Medica Instrument Mfg. Co., India). After 24 h, 1 ml aliquot was withdrawn from each medium and centrifuged at 10,000g for 10 min. Further, the supernatant was filtered (Millex-HV Syringe Filter Unit, 0.45  $\mu$ m, PVDF, 33 mm, gamma sterilized), suitably diluted with the mobile phase and analyzed by the HPLC method.

#### 2.6. In vitro release study

**In vitro** release profiles of GEM-PC and GEM were obtained by the dialysis method (Joshi et al., 2014). Dispersion of GEM-PC and GEM solution was filled inside the dialysis bag (MWCO 10 kDa, Sigma-Aldrich Co., St. Louis, MO, USA) which was then tied from both ends. These bags contain 2 mg of the drug and its equivalent, were then placed in vials containing release media (20 ml of pH 7.4). These vials were incubated in reciprocal shaking water bath maintained at 37 °C/100 rpm for 24 h. At regular time intervals, 1 ml of external release medium was withdrawn and replaced with the same amount of fresh medium. The amount of drug released was then analyzed in the samples by using RP-HPLC and percent cumulative release was plotted v/s time.

#### 2.7. In vitro plasma stability study

Rat plasma (1 ml) was incubated with 0.2 mg of GEM and GEM-PC (in PBS; equivalent to 0.2 mg of GEM) for 24 h. At regular time intervals, 100  $\mu$ l plasma samples were removed and analyzed GEM and its degradation product (2',2'-difluorodeoxyuridine; dFdU) for establishing stability of drug in plasma. Total plasma volume was kept constant by replacing with equal volume of fresh plasma. Briefly, 20  $\mu$ l of tetrahydrouridine (1 mg/ml) was added to 100  $\mu$ l of plasma to inhibit cytidine deaminase. Further, 25  $\mu$ l of an aqueous solution of internal standard (IS; 2' deoxycytidine, 10  $\mu$ g/ml) was added to plasma sample and was vortexed. To extract GEM from plasma, 50  $\mu$ l of 20% trichloroacetic acid was added and the mixture was thoroughly vortexed prior to centrifugation at 5000 rpm for 5 min. The extraction procedure was repeated for better recovery. The combined supernatant was collected and analyzed using RP-HPLC.

Chromatographic separations were attained with RP-HPLC (Waters 2695 separation module, Waters Co., MA, USA) using C18 column (250mm × 4.6mm × 5  $\mu$ m; Thermo Fisher Scientific Inc., USA) and mobile phase (Acetate buffer (pH 5.0, 0.02 M): ACN; 97:3) flowing at 1 ml/min in isocratic mode. Injection volume was kept at 60 ml. GEM and IS were detected at 272 nm ( $\lambda_{\text{max}}$ ) using PDA detector (Waters 2996 photodiode array, Waters Co., MA, USA).

#### 2.8. In silico estimation of complexation

##### 2.8.1. Establishment of the complexation profile via static lattice atomistic simulations (SLAS)

All modeling procedures and computations in vacuum, including energy minimizations in Molecular Mechanics (MM), were performed using HyperChem<sup>TM</sup> 8.0.8 Molecular Modeling Software (Hypercube Inc., Gainesville, FL, USA) and ChemBio3D Ultra 11.0 (CambridgeSoft Corporation, Cambridge, UK). The 3D structure of GEM and the phospholipid was archetyped using ChemBio3D Ultra with natural bond angles. The models were primarily energy-minimized employing the AMBER 3 (Assisted Model Building and Energy Refinements) Force Field algorithm in HyperChem<sup>TM</sup> 8.0.8. The conformer having the lowest energy was used to develop the drug-phospholipid complex. The complex was assembled by parallel disposition and the energy-minimization was repeated to generate the final model: GEM-PC. Full geometrical optimization was conducted in vacuum employing the Polak-Ribiere Conjugate Gradient method until an RMS gradient of 0.001 kcal/mol was reached (Kumar et al., 2012).

##### 2.8.2. Molecular dynamics (MD) simulations

The polymer chains initially minimized by MM were then minimized by molecular dynamics for 1.0 ps (time step = 0.001 ps) at 300 K with the Nose–Hoover thermostat. For evaluation of the stability of a simulation and the extent of equilibration and for identification of the interesting low energy conformations, molecular dynamics calculations were averaged and saved as kinetic energy (EKIN), potential energy (EPOT), total energy (ETOT) and temperature (TEMP). Equilibrium was established before recording the measurements wherein the instantaneous potential and kinetic energy were monitored to determine when the system reaches equilibrium. Thereafter, the simulation was allowed to run for 1000 time-steps before taking measurements (Ngwuluka et al., 2015).

#### 2.9. In vitro cell line experiments

##### 2.9.1. Quantitative uptake

MIA PaCa-2, PANC-1 cells were cultured at a density of 10<sup>5</sup> cells/well in 24 well cell culture plates (Costars, Corning Inc., NY, USA)

and allowed to attach overnight. The cell culture medium was replaced with fresh medium containing varying concentration of free GEM, and GEM-PC and further incubated for 2 h to evaluate the concentration dependent effect on cell uptake. Upon completion of incubation period, the medium was removed and cells were washed twice with PBS (pH 7.4). Similarly, time dependent cell uptake studies were also performed by incubating the MIA PaCa-2, PANC-1 cells with appropriate concentration of different formulations for varying time intervals (0.5, 1, 1.5, 2, 4 h). Further cells were lysed with the 0.1% Triton™ X-100 followed by extraction with methanol to completely solubilize the internalized drug. The cell lysate was centrifuged (Sigma K 300, USA) at 18,000 rpm for 10 min and obtained supernatant was subjected to HPLC analysis for quantification of internalized drugs.

#### 2.9.2. Cell cytotoxicity

The cell cytotoxicity of GEM-PC, GEM and blank phospholipid was determined using MTT assay in MIA PaCa-2, PANC-1 (human pancreas adenocarcinoma) cell lines by our previously reported protocol (Swarnakar et al., 2013). Briefly, cells were grown in DMEM, accompanied with Earle's salts, L-glutamine, nonessential amino acids, sodium bicarbonate, sodium pyruvate, 10% FBS, 100 U/ml penicillin, and 100 mg/ml streptomycin and maintained under 5% CO<sub>2</sub> atmosphere at 37 °C. Cells were harvested by using 0.25% w/v trypsin-EDTA solution, sub-cultured in 96-well culture plate (Costars, Corning Inc., NY, USA) at a density of 10<sup>4</sup> cells/well and incubated with different equivalent concentrations (0.1, 1, 10 and 20 µg/ml) of GEM-PC, free drug and blank phospholipids. The extent of viability of the cells is indicated by conversion of MTT to purple colored formazan crystals by metabolically active cells. These needle shape formazan crystals were then solubilized with DMSO (dimethyl sulphoxide) and optical density was measured at 540 nm spectrophotometrically. The cell viability was evaluated by following equation:

$$\text{Relative cell viability} = \frac{(\text{Absorbance of sample}) \times 100}{(\text{Absorbance of control})} \quad (1)$$

#### 2.9.3. Apoptosis

The cell cytotoxicity potential of the GEM and GEM-PC were further assessed as a function of their capability to induce apoptosis in MIA PaCa-2 and PANC-1 cells. Standard phosphatidyl serine externalization assay based on Annexin V binding was monitored to estimate the apoptosis (Jain et al., 2014a). Briefly, MIA PaCa-2 and PANC-1 cells were seeded at a density of 10<sup>5</sup> cells per well in the six-well tissue culture plate (Costars, Corning Inc., NY, USA) and allowed to attach overnight at 37 °C and 5% CO<sub>2</sub>. The media was aspirated and cells were exposed to fresh media containing GEM and GEM-PC, equivalent to 1 mg/ml and incubated for 6 h. After incubation, the cells were washed with PBS (2 times) and double stained with Annexin V Cy3.18 conjugate (AnnCy3) and 6-carboxyfluorescein diacetate (6-CFDA) following the manufacturer's protocol (Annexin V-Cy3™ Apoptosis Detection Kit, Sigma, USA). Cells were then visualized under confocal laser scanning microscope (CLSM; Olympus FV1000, Olympus Imaging America Inc., USA) with green (for 6-CFDA) and red (for AnnCy3) channels. The cells stained with different fluorescence were categorized as live (green), apoptotic (red and green) and necrotic (green). Apoptosis index, the ratio of the fluorescence intensity of the red fluorescence (originated from the Annexin V Cy3.18 conjugate, estimate of apoptosis) to the fluorescence intensity of green fluorescence (originated from the 6-carboxyfluorescein, estimate of viable cells) was also calculated for the GEM and GEM-PC. The quantitative evaluation of fluorescence within the images could be determined by processing images with Image J software (U.S.

National Institutes of Health, Bethesda, Maryland, USA, <http://imagej.nih.gov/ij/>).

#### 2.10. In vivo pharmacokinetics

The pharmacokinetics of GEM, GEM-PC and GEMITA (Fresenius Kabi India Pvt. Ltd., India, Sterile lyophilized powder for Injection in a 10 ml vial containing 200 mg of gemcitabine (base)) was performed in male Sprague Dawley rats (150–180 g), fasted overnight. Animal study protocol was duly approved by the Institutional Animal Ethics Committee (IAEC), National Institute of Pharmaceutical Education & Research (NIPER), India. The rats were randomly divided into 3 groups of 5 animals each. Animal were administered with free GEM (10 mg/kg) and formulations (GEM-PC and GEMITA; equivalent to 10 mg/kg GEM) administered intravenously (after reconstitution in sterile water for injection) via tail vein. Blood samples (250 µl) were collected, from tail vein in the heparinized micro-centrifuge tubes at periodic intervals of 0, 0.5, 1, 1.5, 2, 3, 4, 6, 8, 12 and 24 h under mild anesthesia. Collected blood samples were centrifuged at 5000 rpm for 5 min to separate the plasma as supernatant. The plasma samples were analyzed for drug content using validated HPLC method, which was explained in previous section.

The pharmacokinetic parameters of GEM-PC were calculated by Kinetica software version 5.0 (Thermo Fisher Scientific Inc., USA), and compared with free GEM and marketed formulation. Maximum concentration (C<sub>max</sub>) and time to reach maximum concentration (T<sub>max</sub>) are the values obtained directly from concentration-time curve. Area under the concentration-time curve (AUC<sub>0–∞</sub>), elimination half-life (t<sub>1/2</sub>), mean residence time (MRT) were determined.

#### 2.11. Toxicity study

##### 2.11.1. In vitro haemolytic study

Whole human blood was collected in heparinized micro-centrifuge tubes and subjected to centrifugation at 2500 rpm for 5 min at 4 °C to separate red blood cells (RBCs). The supernatant along with buffy clot was discarded and RBCs were washed thrice with isotonic PBS, pH 7.4. The stock of RBCs was prepared to a concentration of 0.1% v/v by mixing with PBS. A 100 µl of 0.1% w/v GEM and its equivalent in GEM-PC were mixed with 1 ml of RBC suspension. RBCs mixed with 0.1% Triton-X® 100 and PBS were employed as positive and negative control, respectively. The samples were incubated at 37 °C for 1 h in a shaker bath and then centrifuged at 2500 rpm for 5 min to separate supernatant, which was allowed to stand at room temperature for 30 min to oxidize hemoglobin (Hb). The absorbance of oxygenated hemoglobin (Oxy-Hb) was measured spectrophotometrically at 540 nm, and percentage haemolysis was calculated by using following equation:

$$\% \text{Haemolysis} = \left( \frac{AB_s}{AB_{100}} \right) \times 100 \quad (2)$$

Where AB<sub>s</sub> is the absorbance of the sample and AB<sub>100</sub> is the absorbance of the positive control.

##### 2.11.2. In vivo toxicity

The *in vivo* toxicity studies were carried out in Swiss albino mice (25–30 g). The animals were randomly divided into three groups containing 5 animals each. The groups were named as, Group I: Vehicle control, Group II: Marketed formulation (GEMITA; GEM) and Group III: Gemcitabine-phospholipid complex. Intravenous dose of equivalent amount of 10 mg/kg of gemcitabine in GEMITA and GEM-PC were administered into mice via tail vein. After 7 days, all mice were humanely sacrificed and their blood was collected in

heparinized microcentrifuge tubes and subjected to centrifugation at 2500 rpm for 5 min at 4 °C to separate red blood cells (RBCs) and plasma. The plasma samples were then evaluated for different toxicity markers like AST, ALT, BUN and Creatinine level by utilizing commercial kits available in the market (Accurex Biomedical Pvt. Ltd., Mumbai, India). Obtained RBCs were studied for their morphological changes under Scanning Electron Microscopy (SEM). Briefly, The RBC pellet obtained was incubated with 0.5% glutaraldehyde solution at 4 °C for one and half hour for fixation. Free glutaraldehyde was separated by centrifugation at 2000 rpm for 5 min and the RBC pellet was washed thrice with distilled water. Final RBC dispersion was imaged under SEM (S-3400, Hitachi Ltd., Japan) at an acceleration voltage of 10 kV. Samples were placed on carbon tape, sputter coated (E-1010, Hitachi Ltd., Japan) with gold-palladium alloy and observed at different magnifications under SEM.

For organ toxicity evaluation, tissue samples of liver, spleen, lung and kidney were collected and fixed in 10% Neutral Buffered Formalin followed by their embedding in paraffin for tissue sectioning. The tissues were stained with hematoxylin and eosin (H&E) for microscopic examination and observed for toxicity markings.

## 2.12. In vivo pharmacodynamic study

*In vivo* efficacy study of the free drug and drug phospholipid complex was studied in chemically induced pancreatic adenocarcinoma model. Sprague Dawley rats, weighing 150–180 g were divided into 4 groups (viz. Group I; vehicle treated healthy group, Group II; negative control, Group III; GEMITA (GEM) treated and Group IV; GEM-PC treated) containing 6 animals each. Initially, pancreatic adenocarcinoma in Sprague Dawley rats was induced by median laparotomy and implanting 9 mg of DMBA into the proximal pancreas followed by suturing. Then, Group III and IV were treated weekly by administering GEMITA and GEM-PC (equivalent to 5 mg/kg of GEM) respectively, via tail vein. The change in body weight of animals was recorded on each day basis. Later, Rats were sacrificed at the end of study after which the excised pancreata was fixed in formalin, embedded in paraffin, and stained with hematoxylin-eosin for histologic analysis. Further, the level of interleukin-6 (IL-6) as an inflammatory marker in serum of treated animals was also evaluated by ELISA using the commercially available diagnostic kits (Ray Biotech Inc. Norcross GA) (Swarnakar et al., 2014). Normalization of IL-6 levels of GEMITA/GEM-PC treated animals was carried out by comparison with that of healthy group and DMBA treated animals.

## 2.13. Statistical analysis

All the results are exhibited here, as mean ± standard deviation (SD). Data was analyzed using student's *t*-test or one-way ANOVA

(GraphPad InStat Software Demo, US); *p*-values <0.05 was considered as statistically significant.

## 3. Results

### 3.1. Preparation of GEM-PC

In this study, phospholipid complex of gemcitabine was prepared by the solvent evaporation method and screened for different parameters, viz. solvent, and drug phospholipid ratio. Initially, different solvents viz. ethanol, tetrahydrofuran and methanol with dielectric constant 24.5, 7.58 and 31.7 respectively, were used for the phospholipid complex formation. It has previously been reported that solvents with higher dielectric constant may actuate a greater change in electric potential and lowers the interactions between the used components (Wu et al., 2001). However, in our work, we found maximum complexation efficiency with ethanol (89.36 ± 5.51%; see Supplementary content) and thus selected it as a final solvent for preparation of GEM-PC. There is a plenty of information related to range of drug: phospholipid ratio used in the formation of phospholipid complex, and it was found in between 1:1 to 1:4 in most of the cases (Li et al., 2011, 2008). Maximum complexation efficiency (89.36 ± 5.51%) and loading efficiency (22.33%) was obtained with 1:1 drug: phospholipid ratio in our case and thus selected for further study.

### 3.2. Characterization of GEM-PC

DSC thermogram of GEM exhibited a sharp endotherm at 275.02 °C which corresponds to its melting endotherm and its crystalline state (Fig. 1(I)). This type of endotherm was also supported by prior art (Joshi et al., 2014). Phospholipid showed two different types of endothermal peaks in thermograms; the first mild endothermal peak appeared at 80.2 °C and the second sharp endothermal peak at 221.49 °C which could probably be due to its transformation from gel state to liquid crystal state (Kasseem et al., 2017). Physical mixture of GEM and phospholipid showed a shifted peak at 236.36 °C with peaks of phospholipid and GEM. The thermogram of the GEM-PC exhibits only a single peak at 79.21 °C.

The PXRD patterns of GEM, phospholipid, their physical mixture and the phospholipid complex are presented in Fig. 1(II). The PXRD pattern of GEM showed the presence of intense, sharp peaks at 9.81 (2θ), 11.48 (2θ), 13.89 (2θ), 19.24 (2θ), 24.08(2θ) and 27.9(2θ) which indicated its crystalline behavior. The PXRD pattern of phospholipid showed no sharp peaks which stipulated its amorphous state. The physical mixture of both components showed crystalline peaks of GEM with reduced intensities on 2θ scale (e.g. 9.8, 13.89 and 19.2). These findings suggested some interactions between GEM and phospholipid.

FT-IR spectra (see Supplementary content) of GEM showed characteristic peaks of N—H bending at 1623 cm<sup>-1</sup>, ureido group at

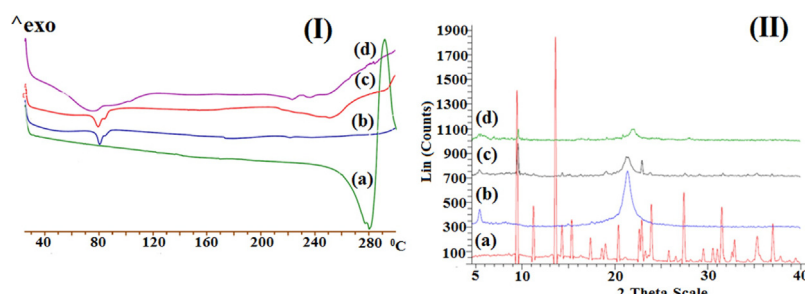


**Fig. 1.** (I) Overlay DSC pattern of GEM (a), phospholipid (b), physical mixture of drug with phospholipid (c), and GEM-PC (d); (II) P-XRD images of GEM (a), phospholipid (b), physical mixture (c), and GEM-PC (d).

1735 cm<sup>-1</sup> and N—H stretching at 3387 cm<sup>-1</sup>. The phospholipid exhibited strong aliphatic phosphate stretching at 1253 cm<sup>-1</sup> and C=O stretching of two long aliphatic chains of fatty acids at 1734 cm<sup>-1</sup> (Han et al., 2000). FT-IR spectrum of the physical mixture had superimposition of the spectra of both components and revealed broadening and shifting of their characteristic peaks, suggested that both had few interactions between them. Further, these characteristic peaks i.e. primary amine of drug and aliphatic phosphate group were either broadened or disappeared and physical mixture of both components showed broadened peak of GEM (3337 cm<sup>-1</sup>), a red shift confirming the formation of new set of interactions revealing hyperconjugation interactions. Further, the shifts in the characteristic absorption band of GEM (1739 cm<sup>-1</sup>; blue shift) and phospholipid (1234 cm<sup>-1</sup>; red shift) in the spectra of physical mixture also exhibited the few interactions between phospholipid and drug (Hou et al., 2012; Li et al., 2008). However, characteristic peaks of GEM (1623 cm<sup>-1</sup>; N—H bending) and phospholipid (1253 cm<sup>-1</sup>; aliphatic phosphate stretching) were disappeared in the GEM-PC spectra. Moreover, spectra of GEM-PC showed blue shift in N—H stretching (3364 cm<sup>-1</sup>) with broadening which meant to have rehybridization type interactions (Joseph and Jemmis, 2007). Overall, these effects support the formation of complexation phenomenon between drug and phospholipid.

In the phospholipid <sup>1</sup>H NMR spectra (see Supplementary data), the protons of methyl group tethered to N-atom [—N<sup>+</sup>(CH<sub>3</sub>)<sub>3</sub>] were indicated by the signals at 3.32 δ (ppm) (Pathan and Bhandari, 2011). The methylene protons near to N-atom (—CH<sub>2</sub>—N<sup>+</sup>), P—O-group (—P—O—CH<sub>2</sub>—) and —C(=O)—C group showed the shift values of 3.45 δ (ppm), 3.62 δ (ppm) and 2.33, respectively. The shift value of 0.85 δ (ppm) was due to the methyl protons of aliphatic side chain, while the value of 1.33 δ (ppm) described the presence of methylene proton of an aliphatic carbon chain of the molecule. <sup>1</sup>H NMR spectrum of GEM exhibited chemical shift of 1° amine or alcohol at 2.11 δ (ppm) and supposed to be merged with —C(=O)—C protons of phospholipid. Aromatic pyrimidine protons of GEM revealed chemical shift δ 3.47 and 3.74 ppm, which were downfielded to 3.79 and 3.82 δ (ppm), respectively with GEM-PC, which was due to aromatic pyrimidine protons. In <sup>31</sup>P NMR spectra (see Supplementary data), chemical shift δ (ppm) of phosphorous in phospholipid showed value of 0.5856, which shifted to 0.5976 in phospholipid complex of GEM confirmed some interactions between phospholipid and GEM. Hence, from both studies (FT-IR and NMR), absence of any new peak or shift omits the probability of chemical interactions.

**Fig. 2(I)** illustrates the SEM images of GEM, phospholipid, physical mixture and GEM-PC. The GEM (**Fig. 2Ia**) and phospholipid (**Fig. 2Ib**) was fully characterized by the sharp crystalline crystals and fused structure respectively. However, physical mixture (**Fig. 2Ic**) comprises both structure but with reduced intensity. But, SEM image of phospholipid complex (**Fig. 2Id**) was characterized with the rough and porous structure which confirmed the absence of crystallinity of GEM (Singh et al., 2011). **Fig. 2(II)** shows the TEM images of GEM-PC, when it was diluted with HPLC water. It appears as a well defined, uniform micellar shape vesicles with an inner dark core surrounded by lighter striations, probably composed of the phospholipid.

### 3.3. Solubility

The solubility data of GEM, physical mixture and GEM-PC in water and *n*-octanol is represented in **Table 1**. Liposolubility of phospholipid complex in *n*-octanol was significantly increased (~16 times) as compared with pure drug and physical mixture. However, it was not significantly enhanced by mere mixing of drug and phospholipid. This indicated the enhancement of liposolubility

of hydrophilic drug, following complexation with phospholipid (Li et al., 2013).

### 3.4. In vitro release

*In vitro* release of GEM and GEM-PC was measured by dialysis method (**Fig. 3(I)**). It was very clear that free GEM solution showed only monophasic release pattern and released most of the drug within 2 h (97.4 ± 7.3%). However, GEM-PC showed biphasic pattern; the initial burst release (42.6 ± 11.8% for 1 h) followed by sustained release profile (67.3 ± 12.1% for 24 h). The mechanism of drug release from GEM-PC was determined by different mathematical models e.g. zero order, first order, Higuchi kinetics and Korsmeyer-Peppas model. Kinetic profiling indicates zero order release with non-Fickian transport in the burst release phase followed by Higuchi kinetics with Fickian transport during the sustained release phase (supplementary Table S2).

### 3.5. In vitro plasma stability

Stability of GEM and GEM-PC in plasma was studied by determining the percentage of analyte (GEM or dFdU) relative to their initial level, after incubation them in rat plasma (**Fig. 3(II)**) for 24 h. Free GEM on incubation with plasma showed a rapid decline in its concentration to 21.8%, within 24 h, which could be due to higher metabolism of free drug (release of dFdU; 68.47%) in plasma by deoxycytidine deaminase. However, in the case of GEM-PC, 48.77% of intact GEM was remained in plasma after 24 h, which is significantly higher than free GEM (*p* < 0.01).

### 3.6. Molecular mechanics assisted model building and energy refinements

Molecular mechanics energy relationship (MMER), a method for analytico-methematical representation of potential energy surfaces, was used to provide information about the contributions of valence terms, noncovalent Coulombic terms, and non covalent van der Waals interactions for gemcitabine/phospholipid interactions. The MMER model for potential energy factor in various molecular complexes can be written as:

$$E_{\text{molecule/complex}} = V_{\Sigma} = V_b + V_{\theta} + V_{\varphi} + V_{ij} + V_{hb} + V_{el} \quad (3)$$

Where,  $V_{\Sigma}$  is related to total steric energy for an optimized structure,  $V_b$  corresponds to bond stretching contributions,  $V_{\theta}$  denotes bond angle contributions,  $V_{\varphi}$  represents torsional contribution arising from deviations from optimum dihedral angles,  $V_{ij}$  incorporates van der Waals interactions due to non-bonded interatomic distances,  $V_{hb}$  symbolizes hydrogen-bond energy function and  $V_{el}$  stands for electrostatic energy.

In addition, the total potential energy deviation,  $\Delta E_{\text{Total}}$ , was calculated as the difference between the total potential energy of the complex system and the sum of the potential energies of isolated individual molecules, as follows:

$$\Delta E_{\text{Total}} = E_{\text{Total}} - [E_{\text{GEM}} + E_{\text{PC}}] \quad (4)$$

The molecular stability can then be estimated by comparing the total potential energies of the isolated and complexed systems. If the total potential energy of complex is smaller than the sum of the potential energies of isolated individual molecules in the same conformation, the complexed form is more stable and its formation is favored (Kumar et al., 2014).

$$\begin{aligned} E_{\text{GEM}} &= 19.441V_{\Sigma} \\ &= 0.731V_b + 10.633V_{\theta} + 5.562V_{\varphi} + 2.514V_{ij} \end{aligned} \quad (5)$$

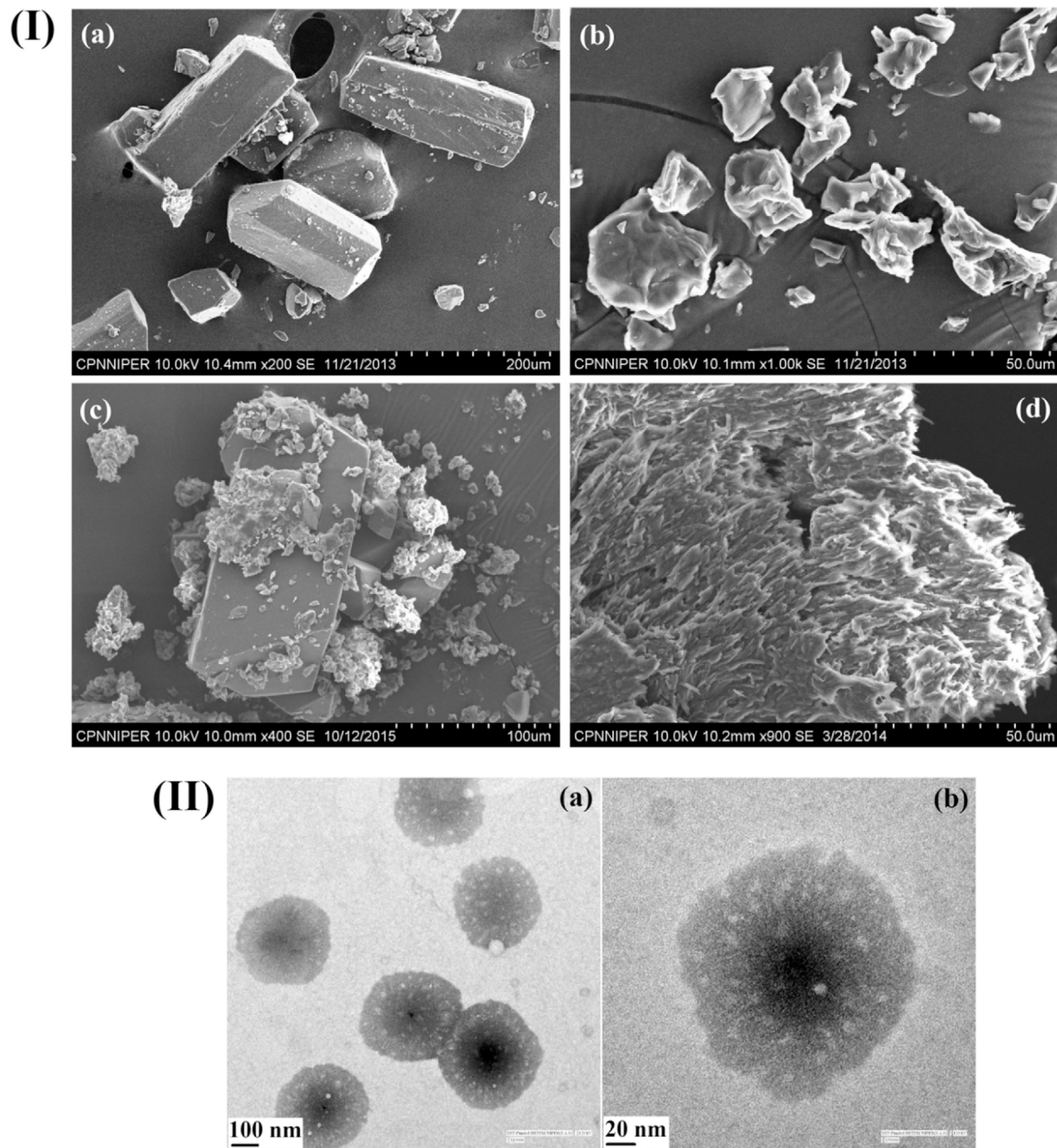


**Fig. 2.** (I) SEM images of GEM (A), phospholipid (B), and GEM-PC (C); (II) TEM photographs of GEM-PC in aqueous dispersion X 19,000 (A), and X 50,000 (B).

$$\begin{aligned} E_{PC} &= 70.985V_{\Sigma} \\ &= 1.662V_b + 58.234V_{\theta} + 28.195V_{\varphi} - 0.975V_{ij} \\ &\quad - 16.132V_{el} \end{aligned} \quad (6)$$

$$\begin{aligned} E_{Total} &= 9.952V_{\Sigma} \\ &= 2.089V_b + 28.064V_{\theta} + 32.123V_{\varphi} - 16.577V_{ij} \\ &\quad - 35.747V_{el} \end{aligned} \quad (7)$$

$$\Delta E_{Total} = -80.474 \text{ kcal/mol} \quad (8)$$

The energetic and geometrical profile of GEM and PC complexation is depicted in Eqs. (5)–(7) and Fig. 4, respectively. The drug-phospholipid complex demonstrated energetic stability

with very high negative energy of formation ( $\Delta E$ ) value of  $\approx 80$  kcal/mol (Eq. (8)) justifying the selection of Lipoid S75 for enhanced lipid solubility and metabolic stability of gemcitabine. Interestingly, the total steric energy for GEM-PC complex ( $V_{\Sigma} = 9.952$  kcal/mol) was even less than that of the drug, gemcitabine ( $V_{\Sigma} = 19.441$  kcal/mol), further confirming the rationale and

**Table 1**  
Solubility of GEM, physical mixture and GEM-PC.

Samples	Solubility in water (μg/ml)	Solubility in n-octanol (μg/ml)
GEM	$264.24 \pm 13.65$	$13.87 \pm 3.68$
Physical mixture	$265.89 \pm 17.52$	$37.05 \pm 10.91$
GEM-PC	$290.83 \pm 14.57$	$226.68 \pm 15.89^{**}$

All values are expressed as mean  $\pm$  SD (n=3).

\*\* indicates  $p < 0.01$ , when compared to GEM.

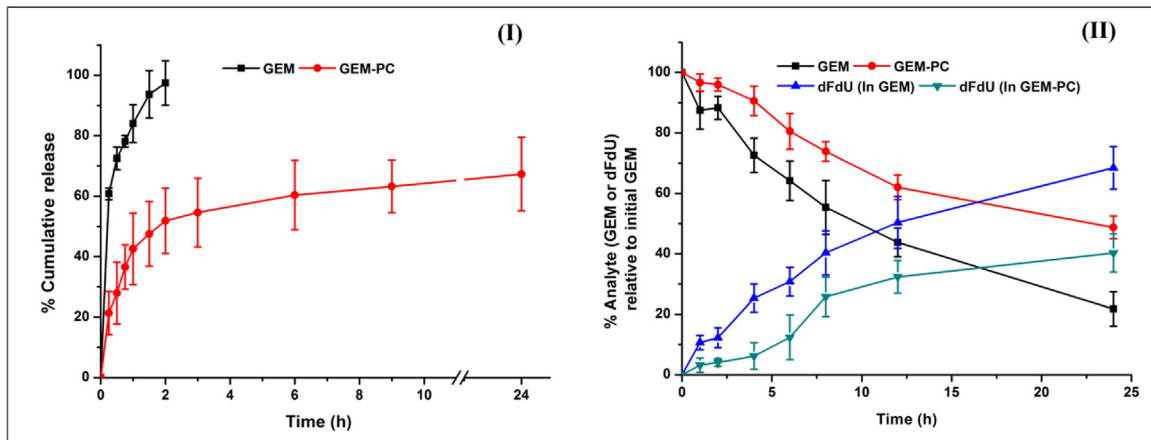


**Fig. 3.** (I) *In vitro* release profile of GEM and GEM-PC; (II) Time dependent concentration of GEM and dFdU, after incubation of GEM and GEM-PC with plasma for 24 h.

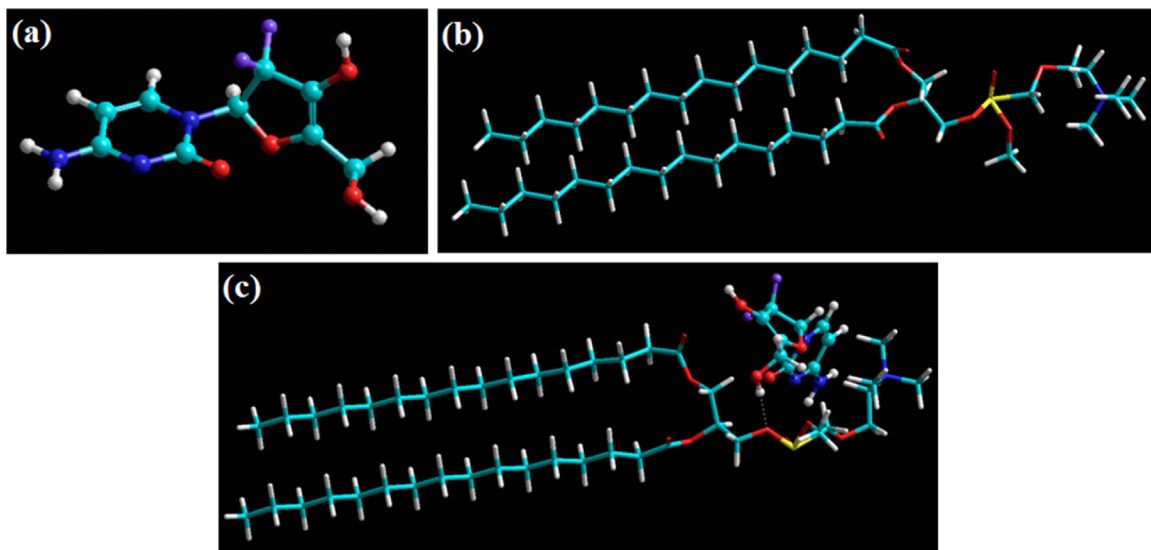


**Fig. 4.** Visualization of geometrical preferences of a) GEM (ball-and-tube rendering), b) PC (tube rendering) and c) GEM-PC after molecular mechanics simulations in vacuum. Standard element color codes: C (cyan), O (red), H (white), P (yellow), N (blue) and F (violet). (For interpretation of the references to colour in this figure legend, the reader is referred to the web version of this article.)

motivation of the current study. From Eqs. (5)–(7); it can be deduced that the GEM-PC molecular complex was stabilized by all bonding ( $V_b$ ,  $V_\varphi$ , and  $V_\theta$ ) and non-bonding ( $V_{ij}$ , and  $V_{ei}$ ) energy contributions with bond angle contributions ( $\Delta E = -40.803 \text{ kcal/mol}$ ), van der Waals forces ( $\Delta E = -15.038 \text{ kcal/mol}$ ) and electrostatic energy ( $\Delta E = -19.615 \text{ kcal/mol}$ ) playing the major role.

To further confirm the geometrical favorability of the drug-phospholipid complex; molecular dynamics calculations were performed. The energetic profile in Table 2 and Fig. S5 confirmed the stabilization of GEM-PC complex by  $\approx 80 \text{ kcal/mol}$  confirming

the results obtained in molecular mechanics simulations. Additionally and importantly, the potential energy of the complex was substantially decreased as compared to the sum of potential energies of the individual components validating our proposition of a stable and tightly bound molecular archetype (Ngwuluka et al., 2015).

### 3.7. In vitro cell line studies

*In vitro* cell cytotoxicity of GEM and GEM-PC was evaluated against PANC-1 and MIA PaCa-2 cells (Human pancreas adenocarcinoma cell lines) by incubating for 24, 48 and 72 h (Fig. 5(I)). A very low or absence of cytotoxicity was observed with only phospholipid treated group which justifies its applicability as a carrier for the newer drug delivery systems. However, GEM-PC revealed significantly higher cytotoxicity (in both cell lines) at all tested time points and the concentration, as compared to free drug (Table 3).

Both time and concentration dependent cell cytotoxicity was analyzed and represented in Fig. 5(II). As the time progresses, more uptake of GEM-PC was estimated. However, after two hours,

**Table 2**  
Energy attributes calculated for the GEM-PC in a molecular dynamics setup.

Molecule	Energy (kcal/mol)		
	EKIN	EPOT	ETOT
GEM	13.290	31.022	44.457
PC	57.702	143.462	201.165
GEM-PC	66.997	98.900	165.898 (-79.724) <sup>a</sup>

<sup>a</sup>  $\Delta E_{\text{Total}(\text{GEM-PC})} = E_{\text{Total}(\text{GEM-PC})} - (E_{\text{Total}(\text{GEM})} + E_{\text{Total}(\text{PC})})$ .

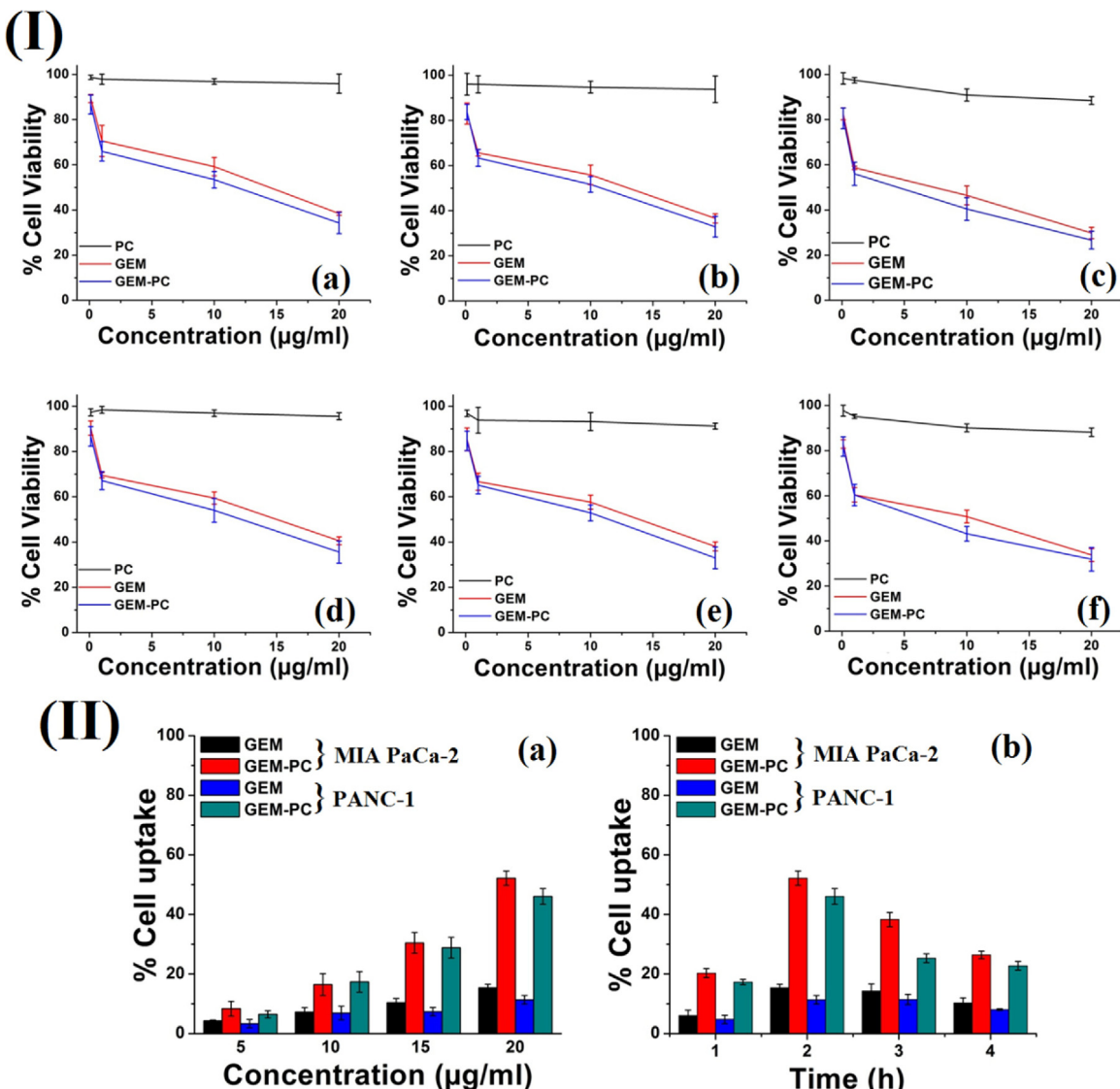


**Fig. 5.** (I) Cell cytotoxicity of blank phospholipid, GEM and GEM-PC at different concentrations; PANC-1 studies (24 h (A), 48 h (B), and 72 h (C)), MIA PaCa-2 studies (24 h (D), 48 h (E), and 72 h (F)); (II) Concentration (A) and Time (B) dependent quantitative cell uptake of GEM and GEM-PC towards MIA PaCa-2 and PANC-1 cell lines;

**Table 3**

$\text{IC}_{50}$  value of GEM and GEM-PC at different time points, when incubated with different cell lines.

Samples	$\text{IC}_{50}$ value ( $\mu\text{g/ml}$ ) in MIA PaCa-2 cells			$\text{IC}_{50}$ value ( $\mu\text{g/ml}$ ) in PANC-1 cells		
	24h	48h	72h	24h	48h	72h
GEM	9.27	6.12	3.7	7.99	5.58	3.62
GEM-PC	5.03	4.26	1.89	5.54	4.43	2.64

uptake of GEM-PC attained a plateau or decline phase which might be due to saturation of receptors (Swarnakar et al., 2013). Furthermore, MIA PaCa-2 showed more sensitivity than PANC-1 cell lines as gemcitabine showed more cytotoxicity against former cell lines than later one. The above results were further validated by the apoptosis assay (Fig. 6). The apoptotic index was observed to be higher in GEM-PC as compared to GEM alone. This outcome has similar pattern in both pancreatic carcinoma cells. The apoptotic index was 0.49 and 0.45 with GEM, which was increased in 0.79 and 0.77, against MIA-PaCa-2 and PANC – 1 cell lines, respectively.

### 3.8. In vivo pharmacokinetics

Fig. 7 illustrates the pharmacokinetic profiles of GEM, GEMITA and GEM-PC. Significant increase in  $\text{AUC}_{0-\infty}$  ( $8983.26 \pm 628.02 \text{ ng h/ml}$ ; ~2 fold,  $p < 0.001$ ) of GEM from GEM-PC was observed when it was compared to  $\text{AUC}_{0-\infty}$  of GEM ( $4371.18 \pm 506.28 \text{ ng h/ml}$ ) and GEMITA ( $4689.29 \pm 710.66 \text{ ng h/ml}$ ) (Table 4). Short half life of GEMITA ( $3.2 \pm 1.4 \text{ h}$ ) was significantly increased in GEM-PC ( $5.4 \pm 0.8 \text{ h}$ ). Permanency (Mean Residence Time; MRT) of drug with phospholipid complex was found ~2 fold higher than GEM and GEMITA ( $p < 0.001$ ).

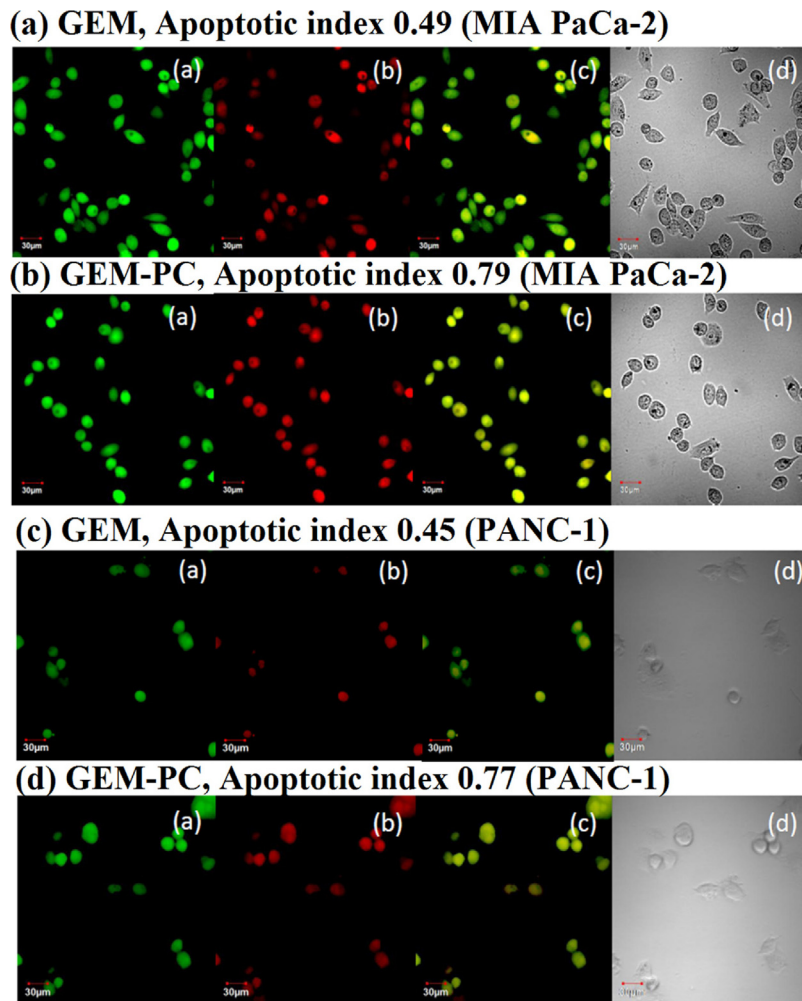


**Fig. 6.** Apoptosis assay of GEM (A) and GEM-PC (B) with PANC-1, and GEM (C) and GEM-PC (D) with MIA PaCa-2 cell lines.

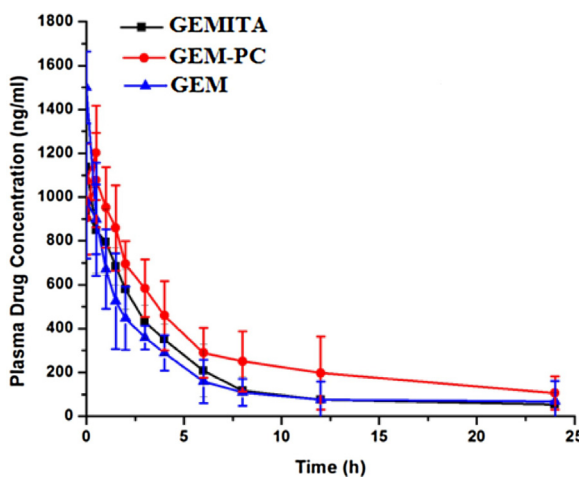


**Fig. 7.** In vivo pharmacokinetic profile of GEM, GEMITA and GEM-PC.

### 3.9. Toxicity studies

#### 3.9.1. In vitro hemolytic study

Fig. 8(I) represents *in vitro* hemolytic toxicity profile of GEM and GEM-PC as compared to positive control of Triton™-X 100 (100%)

and negative control of PBS ( $3.89 \pm 1.67\%$ ). As can be seen from the results, GEM ( $31.28 \pm 5.15\%$ ) showed marked toxicity, whereas GEM-PC ( $19.27 \pm 4.37\%$ ) showed significantly less toxicity as compared to GEM, which could be due to micellar structure attained by GEM-PC and further less exposure to RBCs (Jain et al., 2012). This validates the higher haemocompatibility of GEM-PC over GEM.

#### 3.9.2. In vivo toxicity

Different biochemical markers were evaluated to show the extent of liver and kidney damage. Significant increase ( $p < 0.001$ ) in levels of biochemical markers (AST, ALT, BUN and creatinine) were observed in the plasma of GEMITA (GEM) receiving group as compared to vehicle control (Fig. 8II). However, non-significant increase in marker levels obtained with GEM-PC represents minimal oxidative stress. Further, RBC morphology as observed by SEM images (Fig. 8III) also confirmed the same pattern of toxicity on RBC morphology. These results also validate the findings obtained in *in vitro* hemolytic study.

Similar pattern of toxicity was also observed in histopathology sections of Spleen, liver, lung and kidney (Fig. 9). GEMITA produced significant histological changes in all four organ tissue, causing splenocyte rupture in spleen, decrease in hepatocyte density in liver and inflammation in kidney and lung tissue (arrow indicates high prevalence). The GEM-PC did not show any such effect on the tissues which demonstrated its safety over GEMITA.

**Table 4**

Pharmacokinetic parameters of GEM, GEMITA and GEM-PC.

Parameters	GEM	GEMITA	GEM-PC
$C_{\max}$ (ng/ml)	983.252 ± 264.38	936.55 ± 213.48	1077.46 ± 215.16
$AUC_{0-\infty}$ (ng.h/ml)	4371.18 ± 506.28	4689.29 ± 710.66	8983.26 ± 628.02 **
$t_{1/2}$ (h)	3.9 ± 1.1	3.2 ± 1.4	5.4 ± 0.8
MRT (h)	5.1 ± 1.3	4.8 ± 0.6	9.8 ± 1.5 *

All values are expressed as mean ± SD (n=5).

\* indicates  $p < 0.01$ , when compared to GEM.\*\* indicates  $p < 0.001$ .

### 3.10. Pharmacodynamics

The histopathological images of pancreas (stained with hematoxylin-eosin) of treated groups are shown in Fig. 10(I). Each treatment group showed varying degree of acute or chronic inflammation, ductal or reactive hyperplasia, ductal cell atypia and adenocarcinoma. There was a particularly high prevalence of ductal hyperplasia, atypia, and dysplasia (arrows in Fig. 10.IA) found in negative control group which indicated the pattern of pancreatic ductal adenocarcinoma. Healthy group animals showed absence of any type of inflammation and hyperplasia. Group with free drug treatment expressed low prevalence of ductal atypia and hyperplasia which was further significantly lowered with drug-

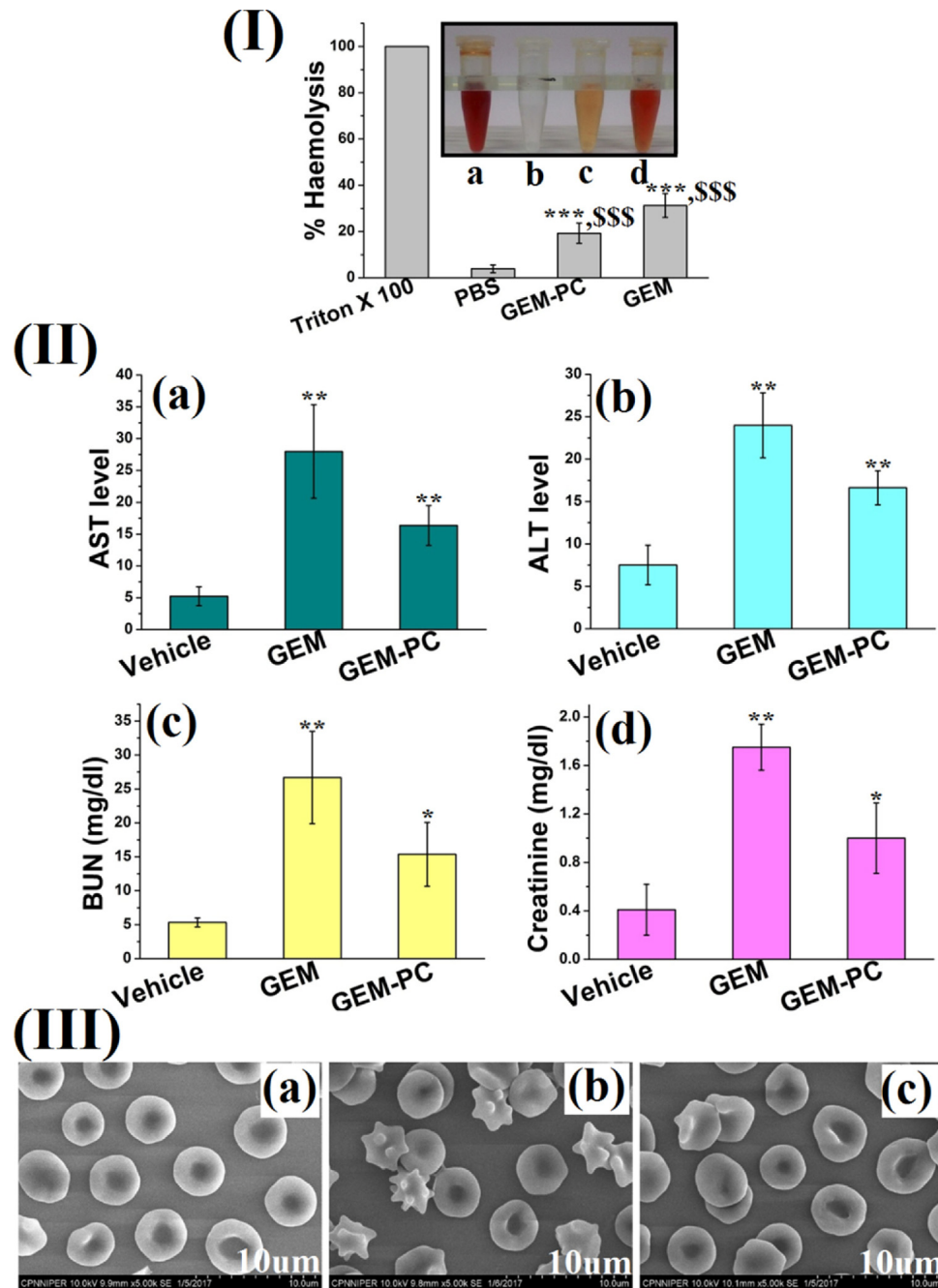


**Fig. 8.** (I) *In vitro* hemolysis assay of various formulations, \*\*\* and \$\$\$ indicates  $p < 0.001$  when compared to Triton™X-100 and PBS respectively; (II) Biochemical markers (A) AST (B) ALT (C) BUN and (D) creatinine levels in plasma, \*\* and \* indicates  $p < 0.01$  and  $p < 0.05$  respectively when compared to Vehicle group; (III) SEM images of RBCs treated with of (A) Vehicle, (B) GEM (GEMITA), and (C) GEM-PC;.

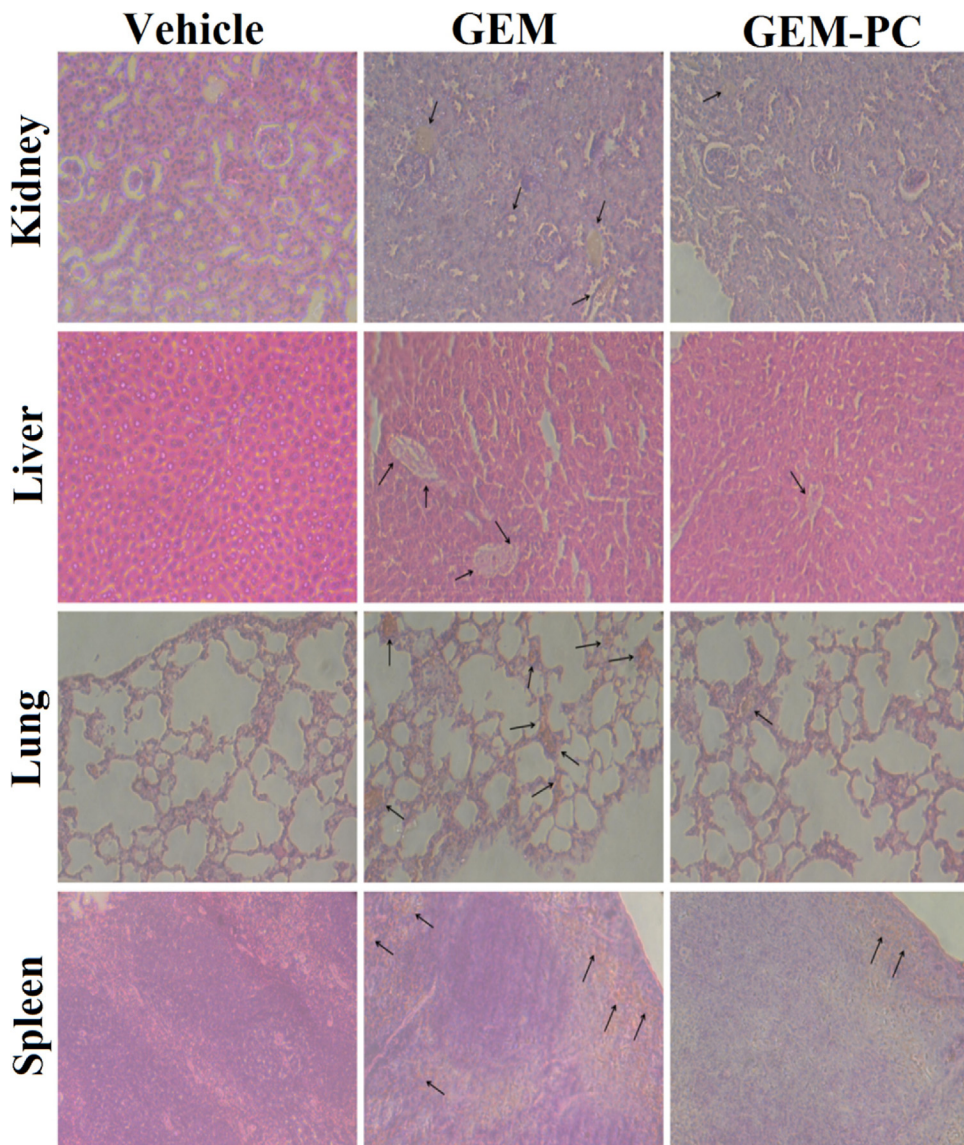


**Fig. 9. (IV)** Histopathological sections of (A) kidney, (B) liver, (C) lung and (D) spleen after treatment of different samples.

phospholipid complex treatment. Further, levels of IL-6 were evaluated to signify the treatment. Fig. 10(II) shows the levels of IL-6 in serum for different groups. The Healthy group (without DMBA) expressed IL-6 value ( $33.46 \pm 9.05$  pg/ml) in the serum, which was significantly lower ( $p < 0.001$ ) than negative group ( $883.38 \pm 50.42$  pg/ml). There was significant decrease ( $p < 0.001$ ) in IL-6 values in case of free drug (GEM) treatment groups than negative control group which were further lowered with GEM-PC. Thus, both histopathology and IL-6 level analysis suggested the improved therapeutic efficacy of GEM-PC over free drug.

#### 4. Discussion

Phospholipid complex technology offers a novel platform for increased efficacy of both hydrophilic as well as lipophilic molecules. With the understanding from previous research, phospholipid complex formation with drug could modify the biopharmaceutical properties, e.g. hydrophilicity and permeability, due to its amphiphilic nature. In this manuscript, phospholipid complex of gemcitabine was successfully prepared to enhance lipid

solubility and metabolic stability of drug. The mechanism of complex formation between drug and phospholipid is not exactly known, but Van der Waals forces and hydrogen bond formation between two components might be the reasons for this type of complexation phenomenon (Lu et al., 2009).

For preparation of successful molecular complex between drug and phospholipid, outcome of screening ratio i.e. 1:1, could be described by the understanding that the polar region of gemcitabine and phospholipid shows enough interactions at this ratio. It might also be due to the low spatial features of gemcitabine at this ratio, and phospholipid successfully envelops the drug molecule with its apolar region without weakening of interactions between two components. With a closer look at the GEM-PC molecular complex, it can be deduced that GEM displayed a “space-filling fit” within the van der Waals space of PC molecule wherein the latter forming a “hook-like archetype” to accommodate the GEM molecule. This can be attributed to significant changes in the bond and dihedral angles of the complex molecule which lead to torsional strain and “geometrical readjustments” in the PC molecule. Furthermore, the van der Waals and electrostatic

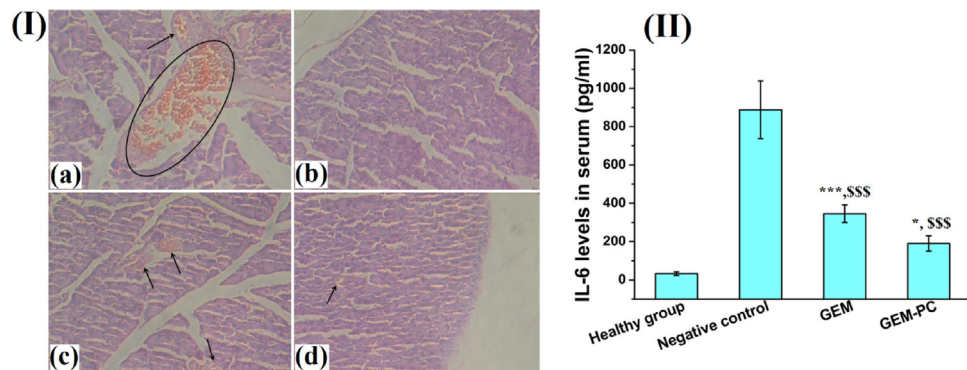


**Fig. 10.** (I) Pathological observation of rat pancreatic lesions (induced by DMBA) of different groups; (A) Negative (B) Healthy group (C) GEM (GEMITA), and (D) GEM-PC treated; (II) IL-6 level in serum (pg/ml) for different groups, \*\*\* and \$\$\$ indicates  $p < 0.001$  when compared to healthy group and negative control respectively. Each value is represented as mean  $\pm$  SD ( $n=5$ ).

interactions lead to a closer fit causing a “molecular merger” and perfect hydrophobic shielding required to attain enhanced lipid solubility and metabolic stability.

Differential scanning calorimetry (DSC) is a quick and sound method to detect possible drug phospholipid interactions. These interactions are resolved by the elimination of endothermic peak(s), appearance of new peak(s), and the change in peak shape and its onset, peak temperature/melting point and relative peak area/enthalpy (Singh et al., 2011). From Fig. 1(I), it is evident that the original peak of GEM disappears from the thermogram of the complex and the phase transition temperature is lower than that of phospholipids, which could be due to some intermolecular interactions between drug and phospholipid. Thus, it confirms the occurrence of the complexation phenomenon between two components, and was also substantiated by Hou et al. (Hou et al., 2012). Disappearance of sharp crystalline peaks of drug in PXRD of GEM-PC (Fig. 1(II)) also confirmed the complex formation which could be due to presence of molecular dispersion or amorphous form of drug in drug phospholipid complex (Shi et al., 2006). Broadening or disappearance of peaks in FTIR study illustrated the complexation phenomenon between two molecular components. In  $^1\text{H}$  NMR (see Supplementary data), changes in chemical shift of characteristic protons confirmed the interactions between drug and phospholipid (Semalty et al., 2012). Sharp single peak of phospholipid complex in  $^{31}\text{P}$  NMR, also validate the absence of bilayer structure which usually formed in liposomal formulation (Leal et al., 2008).

*In vitro* release pattern depicts the basic knowledge about the fabric and the behavior of the formulation at the molecular level. Initial burst and later sustained release pattern was observed with GEM-PC (Fig. 3(I)), which could be due to presence of certain amount of free GEM-PC for initial fast release and GEM-PC associated micellar structure for later prolonged release phenomenon (Hou et al., 2012). Despite the hydrophilicity of GEM, the drug release was slower and sustained, as the drug molecules were interacted with phospholipid molecules with electrostatic/van der Waal's attractions. This transport would be a type of diffusion controlled mechanism, where drug detach from the phospholipid first and slowly diffuses to outer compartment from the micellar body. The slower release of drug from the phospholipid complex could also be explained that lipophilicity of GEM was significantly enhanced by the formation of GEM-PC, thus facilitating the release retardation behavior of hydrophilic GEM (Kassem et al., 2017). Free GEM is much known to metabolize rapidly to dFdU, when given by i.v. dose. To establish stability of GEM as a molecular complex with phospholipid, we performed *in vitro* plasma stability. Current findings from *in vitro* plasma stability studies, depicted the ability

of phospholipid complexation to protect GEM against enzyme mediated degradation in plasma, as previous findings with conjugation phenomenon corroborated the similar results (Das et al., 2014; Jain et al., 2014b).

The higher cell cytotoxicity of GEM-PC was observed in *in vitro* cell studies, which could be explained by better cellular uptake of GEM-PC as compared to free drug (Wei et al., 2010), which was also confirmed by *in vitro* quantitative cell uptake experiment and sustained release behavior. Overall, cell uptake of GEM-PC was found higher as compared to free GEM which could be due to more endocytosis and internalization of GEM-PC (Dora et al., 2016).

*In vivo* toxicity studies also supported the results observed with *in vitro* cell culture experiments. As it is well known that conventional gemcitabine therapy is associated with various adverse events to the healthy tissues (Brodowicz et al., 1997; Robinson et al., 2003). Thus, it was essential to evaluate the safety of GEM-PC towards healthy tissues with appropriate model. We selected Swiss mice over rat model because of its better immunogenicity and immunosensitivity. Evaluation of biochemical markers, histopathology of different organs and RBCs morphology were noted to show the extent of safety of GEM-PC over GEMITA or GEM (Jain et al., 2012). Based on these observations, it was concluded that molecular complexation with phospholipid plays an important tool to circumvent the toxicity aspects of drug.

From *in vivo* pharmacokinetics,  $\sim 2$  fold increase in  $AUC_{0-\infty}$  was found with GEM-PC than free drug and marketed formulation. The increase in AUC could be due to formation of drug phospholipid complex associated micellar structure, which provided protection to the drug against enzymatic deactivation (Li et al., 2014; Song et al., 2008). Increase in residence time ( $\sim 2$  fold) of GEM-PC was also observed, which can be explained by higher lipid solubility of GEM-PC. *In vivo* efficacy study was determined to validate the improved pharmacodynamics of GEM-PC, which could be explained by different ways (1) enhancement of lipophilicity by complexation and increased access to the internal environment of cancer cells, (2) Prolonged exposure of molecular complex as explained by higher plasma stability and MRT, and (3) Uptake of molecular complex by endocytosis due to micellar structure formed when intravenously administered. *In vivo* efficacy results were further corroborated with inflammatory marker. From literature, it is well documented that excessive production of IL-6 is involved in the pathogenesis of acute pancreatitis and blockade of IL-6 accelerates acinar cell apoptosis (Chao et al., 2006; Norman et al., 1997). So, the present study described the usefulness of molecular complex of GEM and phospholipid as a superior platform in terms of stability, toxicity and efficacy.

## 5. Conclusion

We have successfully developed Phospholipid complex of GEM primarily to enhance lipid solubility (~13 times). Complexation phenomenon was able to transform the physicochemical and pharmacological properties of drug. Our findings based on *in vitro* and *in silico* studies clearly demonstrated the superiority of GEM-PC over free drug. Prospectives of phospholipid complex was clearly seen with higher cytotoxicity found with pancreatic adenocarcinoma cell lines. Further, *in vivo* pharmacokinetic (~2 times higher AUC), safety (~1.6 times lower haemolysis) and efficacy studies confirmed the potential of drug phospholipid complex. Furthermore, long term toxicity and clinical studies are needed to explore the full potential of phospholipid complexation phenomenon.

## Acknowledgements

The authors are thankful to Mac-Chem products (India) Pvt. Ltd. (Mumbai, India) for providing gift samples of Gemcitabine hydrochloride. Authors are thankful to Director, NIPER, S.A.S. Nagar for providing the necessary infrastructure facilities. Chander Parkash and Varun Kushwah are also thankful to University Grants Commission (UGC), New Delhi and Council of Scientific and Industrial Research (CSIR), New Delhi respectively for financial assistance. The help and co-operation provided by Mr. Rahul Mahajan and Mr. Vinod, NIPER, S.A.S. Nagar for SEM and TEM analysis respectively, is duly acknowledged.

## Appendix A. Supplementary data

Supplementary data associated with this article can be found, in the online version, at <http://dx.doi.org/10.1016/j.ijpharm.2017.07.060>.

## References

- Arias, J.L., Reddy, L.H., Couvreur, P., 2011. Superior preclinical efficacy of gemcitabine developed as chitosan nanoparticulate system. *Biomacromolecules* 12, 97–104.
- Brodowicz, T., Wiltschke, C., Zieliński, C.C., Breiteneder, S., 1997. Gemcitabine-induced hemolytic uremic syndrome: a case report. *J. Natl. Cancer Inst.* 89, 1895–1896.
- Chao, K.C., Chao, K., Chuang, C., Liu, S., 2006. Blockade of interleukin 6 accelerates acinar cell apoptosis and attenuates experimental acute pancreatitis *in vivo*. *Br. J. Surg.* 93, 332–338.
- Daman, Z., Ostad, S., Amini, M., Gilani, K., 2014. Preparation, optimization and *in vitro* characterization of stearoyl-gemcitabine polymeric micelles: a comparison with its self-assembled nanoparticles. *Int. J. Pharm.* 468, 142–151.
- Das, M., Jain, R., Agrawal, A.K., Thanki, K., Jain, S., 2014. Macromolecular bipill of gemcitabine and methotrexate facilitates tumor-specific dual drug therapy with higher benefit-to-risk ratio. *Bioconjug. Chem.* 25, 501–509.
- Dasanu, C.A., 2008. Gemcitabine: vascular toxicity and prothrombotic potential. *Expert Opin. Drug Saf.* 7, 703–716.
- Desmaële, D., Gref, R., Couvreur, P., 2012. Squalenoylation: a generic platform for nanoparticulate drug delivery. *J. Control. Release* 161, 609–618.
- Dhanikula, A.B., Panchagnula, R., 2008. Fluorescence anisotropy, FT-IR spectroscopy and 31-P NMR studies on the interaction of paclitaxel with lipid bilayers. *Lipids* 43, 569–579.
- Dora, C.P., Trotta, F., Kushwah, V., Devasari, N., Singh, C., Suresh, S., Jain, S., 2016. Potential of erlotinib cyclodextrin nanosponge complex to enhance solubility, dissolution rate, *in vitro* cytotoxicity and oral bioavailability. *Carbohydr. Polym.* 137, 339–349.
- Duan, M., Zhou, H., Yan, Z., 2013. Nanoemulsion of resveratrol-phospholipid complex and method for preparing the same and applications thereof. US Patent (US 8465757 B2).
- Han, Y., Zhou, Y., Zhao, Y., 2000. The purification and the identification of lecithin and its application. *Amino Acids Biotic Resour.* 23, 28–31.
- Hou, Z., Li, Y., Huang, Y., Zhou, C., Lin, J., Wang, Y., Cui, F., Zhou, S., Jia, M., Ye, S., 2012. Phytosomes loaded with mitomycin C-soybean phosphatidylcholine complex developed for drug delivery. *Mol. Pharm.* 10, 90–101.
- Immordino, M.L., Brusa, P., Rocco, F., Arpicco, S., Ceruti, M., Cattel, L., 2004. Preparation, characterization, cytotoxicity and pharmacokinetics of liposomes containing lipophilic gemcitabine prodrugs. *J. Control. Release* 100, 331–346.
- Jain, S., Valvi, P.U., Swarnakar, N.K., Thanki, K., 2012. Gelatin coated hybrid lipid nanoparticles for oral delivery of amphotericin B. *Mol. Pharm.* 9, 2542–2553.
- Jain, A.K., Thanki, K., Jain, S., 2014a. Novel self-nanoemulsifying formulation of quercetin: implications of pro-oxidant activity on the anticancer efficacy. *Nanomedicine* 10, 959–969.
- Jain, S., Jain, R., Das, M., Agrawal, A.K., Thanki, K., Kushwah, V., 2014b. Combinatorial bio-conjugation of gemcitabine and curcumin enables dual drug delivery with synergistic anticancer efficacy and reduced toxicity. *RSC Adv.* 4, 29193–29201.
- Jena, S.K., Singh, C., Dora, C.P., Suresh, S., 2014. Development of tamoxifen-phospholipid complex: novel approach for improving solubility and bioavailability. *Int. J. Pharm.* 473, 1–9.
- Joseph, J., Jemmis, E.D., 2007. Red-, blue-, or no-shift in hydrogen bonds: a unified explanation. *J. Am. Chem. Soc.* 129, 4620–4632.
- Joshi, G., Kumar, A., Sawant, K., 2014. Enhanced bioavailability and intestinal uptake of Gemcitabine HCl loaded PLGA nanoparticles after oral delivery. *Eur. J. Pharm. Sci.* 60, 80–89.
- Kassem, A.A., El-Alim, S.H.A., Basha, M., Salama, A., 2017. Phospholipid complex enriched micelles: a novel drug delivery approach for promoting the antidiabetic effect of repaglinide. *Eur. J. Pharm. Sci.* 99, 75–84.
- Khan, J., Alexander, A., Saraf, S., Saraf, S., 2013. Recent advances and future prospects of phyto-phospholipid complexation technique for improving pharmacokinetic profile of plant actives. *J. Control. Release* 168, 50–60.
- Khatik, R., Dwivedi, P., Shukla, A., Srivastava, P., Rath, S.K., Paliwal, S.K., Dwivedi, A.K., 2016. Development, characterization and toxicological evaluations of phospholipid complexes of curcumin for effective drug delivery in cancer chemotherapy. *Drug Deliv.* 1–12.
- Kiew, L.V., Cheong, S.K., Sidik, K., Chung, L.Y., 2010. Improved plasma stability and sustained release profile of gemcitabine via polypeptide conjugation. *Int. J. Pharm.* 391, 212–220.
- Kumar, P., Choonara, Y.E., Toit, L.C.D., Modi, G., Naidoo, D., Pillay, V., 2012. Novel high-viscosity polyacrylamidated chitosan for neural tissue engineering: fabrication of anisotropic neurodurable scaffold via molecular disposition of persulfate-mediated polymer slicing and complexation. *Int. J. Mol. Sci.* 13, 13966–13984.
- Kumar, P., Choonara, Y.E., Pillay, V., 2014. In silico affinity profiling of neuroactive polyphenols for post-traumatic calpain inactivation: a molecular docking and atomistic simulation sensitivity analysis. *Molecules* 20, 135–168.
- Leal, C., Rognvaldsson, S., Fossheim, S., Nilssen, E.A., Topgaard, D., 2008. Dynamic and structural aspects of PEGylated liposomes monitored by NMR. *J. Colloid Interface Sci.* 325, 485–493.
- Li, Y., Yang, D.J., Chen, S.L., Chen, S.B., Chan, A.S.C., 2008. Comparative physicochemical characterization of phospholipids complex of puerarin formulated by conventional and supercritical methods. *Pharm. Res.* 25, 563–577.
- Li, N., Ye, Y., Yang, M., Jiang, X., Ma, J., 2011. Pharmacokinetics of baicalin-phospholipid complex in rat plasma and brain tissues after intranasal and intravenous administration. *Pharmazie* 66, 374–377.
- Li, Y., Jin, W., Yan, H., Liu, H., Wang, C., 2013. Development of intravenous lipid emulsion of vinorelbine based on drug-phospholipid complex technique. *Int. J. Pharm.* 454, 472–477.
- Li, Y., Wu, H., Yang, X., Jia, M., Li, Y., Huang, Y., Lin, J., Wu, S., Hou, Z., 2014. Mitomycin C-soybean phosphatidylcholine complex-loaded self-assembled PEG-lipid-PLA hybrid nanoparticles for targeted drug delivery and dual-controlled drug release. *Mol. Pharm.* 11, 2915–2927.
- Lu, Y., Zhang, Y., Yang, Z., Tang, X., 2009. Formulation of an intravenous emulsion loaded with a clarithromycin-phospholipid complex and its pharmacokinetics in rats. *Int. J. Pharm.* 366, 160–169.
- Ngwuluka, N.C., Choonara, Y.E., Kumar, P., du Toit, L.C., Khan, R.A., Pillay, V., 2015. A novel pH-responsive interpolyelectrolyte hydrogel complex for the oral delivery of levodopa. Part I. IPEC modeling and synthesis. *J. Biomed. Mater. Res. Part A* 103, 1077–1084.
- Norman, J.G., Fink, G.W., Denham, W., Yang, J., Carter, G., Sexton, C., Falkner, J., Gower, W.R., Franz, M.G., 1997. Tissue-Specific cytokine production during experimental acute pancreatitis (a probable mechanism for distant organ dysfunction). *Dig. Dis. Sci.* 42, 1783–1788.
- Paolino, D., Cosco, D., Racanicchi, L., Trapasso, E., Celia, C., Iannone, M., Puxeddu, E., Costante, G., Filetti, S., Russo, D., 2010. Gemcitabine-loaded PEGylated unilamellar liposomes vs GEMZAR®: biodistribution, pharmacokinetic features and *in vivo* antitumor activity. *J. Control. Release* 144, 144–150.
- Pappas, P., Mavroudis, D., Nikolaidou, M., Georgoulas, V., Marselos, M., 2006. Coadministration of oxaliplatin does not influence the pharmacokinetics of gemcitabine. *Anticancer Drugs* 17, 1185–1191.
- Pathan, R.A., Bhandari, U., 2011. Preparation & characterization of embelin-phospholipid complex as effective drug delivery tool. *J. Inclusion Phenom. Macrocycl. Chem.* 69, 139–147.
- Peng, Q., Zhang, Z.R., Gong, T., Chen, G.Q., Sun, X., 2012. A rapid-acting, long-acting insulin formulation based on a phospholipid complex loaded PHBHHx nanoparticles. *Biomaterials* 33, 1583–1588.
- Robinson, K., Lambiase, L., Li, J., Monteiro, C., Schiff, M., 2003. Case report: fatal cholestatic liver failure associated with gemcitabine therapy. *Dig. Dis. Sci.* 48, 1804–1808.
- Semalty, A., Semalty, M., Rawat, B.S., Singh, D., Rawat, M., 2009. Pharmacosomes: the lipid-based new drug delivery system. *Expert Opin. Drug Deliv.* 6, 599–612.
- Semalty, A., Semalty, M., Singh, D., Rawat, M., 2012. Phyto-phospholipid complex of catechin in value added herbal drug delivery. *J. Inclusion Phenom. Macrocycl. Chem.* 73, 377–386.
- Shi, K., Cui, F., Yu, Y., Zhang, L., Tao, A., Cun, D., 2006. Preparation and characterization of a novel insulin-phospholipid complex. *Asian J. Pharm. Sci.* 1, 168–174.

- Singh, D., Rawat, M., Semalty, A., Semalty, M., 2011. Emodin-phospholipid complex: a potential of herbal drug in the novel drug delivery system. *J. Therm. Anal. Calorim.* 108, 289–298.
- Singh, C., Bhatt, T.D., Gill, M.S., Suresh, S., 2014. Novel rifampicin-phospholipid complex for tubercular therapy: synthesis, physicochemical characterization and in-vivo evaluation. *Int. J. Pharm.* 460, 220–227.
- Sloat, B.R., Sandoval, M.A., Li, D., Chung, W.-G., Lansakara-P, D.S., Proteau, P.J., Kiguchi, K., DiGiovanni, J., Cui, Z., 2011. In vitro and in vivo anti-tumor activities of a gemcitabine derivative carried by nanoparticles. *Int. J. Pharm.* 409, 278–288.
- Song, Y., Zhuang, J., Guo, J., Xiao, Y., Ping, Q., 2008. Preparation and properties of a silybin-phospholipid complex. *Pharmazie* 63, 35–42.
- Swarnakar, N.K., Thanki, K., Jain, S., 2013. Effect of co-administration of CoQ10-loaded nanoparticles on the efficacy and cardiotoxicity of doxorubicin-loaded nanoparticles. *RSC Adv.* 3, 14671–14685.
- Swarnakar, N.K., Thanki, K., Jain, S., 2014. Enhanced antitumor efficacy and counterfeited cardiotoxicity of combinatorial oral therapy using Doxorubicin- and Coenzyme Q10-liquid crystalline nanoparticles in comparison with intravenous Adriamycin. *Nanomedicine* 10, 1231–1241.
- Vandana, M., Sahoo, S.K., 2010. Long circulation and cytotoxicity of PEGylated gemcitabine and its potential for the treatment of pancreatic cancer. *Biomaterials* 31, 9340–9356.
- Wei, W., Shi, S.J., Liu, J., Sun, X., Ren, K., Zhao, D., Zhang, X.N., Zhang, Z.R., Gong, T., 2010. Lipid nanoparticles loaded with 10-hydroxycamptothechin-phospholipid complex developed for the treatment of hepatoma in clinical application. *J. Drug Target* 18, 557–566.
- Wu, J., Chen, D., Liu, Y., 2001. Study on the preparation of baicalin complex with phospholipid. *Zhongguo Zhong yao za zhi* 26, 166–169.
- Xu, K., Liu, B., Ma, Y., Du, J., Li, G., Gao, H., Zhang, Y., Ning, Z., 2009. Physicochemical properties and antioxidant activities of luteolin-phospholipid complex. *Molecules* 14, 3486–3493.
- Zhang, J., Peng, Q., Shi, S., Zhang, Q., Sun, X., Gong, T., Zhang, Z., 2011. Preparation, characterization, and in vivo evaluation of a self-nanoemulsifying drug delivery system (SNEDDS) loaded with morin-phospholipid complex. *Int. J. Nanomed.* 6, 3405.